Journal of the Korean Ceramic Society
Vol. 42, No. 5, pp. 299~303, 2005.

Effect of $DyFeO_3$ Addition on Crystal Structure and Ferrcelectricity of the $BiFeO_3$-$PbTiO_3$ System

Jeong Seog Kim,† Jong-Uk Kwon, and Chae Il Cheon*

Department of Digital Display Engineering, Hoseo University, Chungnam 336-795, Korea
**Department of Materials Science and Engineering, Hoseo University, Chungnam 336-795, Korea*
(Received March 2, 2005; Accepted May 13, 2005)

ABSTRACT

The crystal structure and ferroelectricity of the (1-x)$BiFeO_3$ (BF)-x$PbTiO_3$ (PT) ceramic system with the addition of $DyFeO_3$ (DF) have been investigated for attaining a high temperature piezoelectric material. This study is focused on the relation between crystal structure and ferroelectric property with the addition of DF over the phase boundary in the (1-x)BF-xPT system. Hysteresis curves of polarization-electric field at room temperature have been measured. The X-ray and neutron diffraction data were analyzed by the rietveld refinement method. The addition of 0.1 mole DF into BF-PT system greatly increases the ferroelectric remanant polarization Pr values, e.g. 17 $\mu C/cm^2$ in 0.6BF-yDF-(0.4-y)PT and 31 $\mu C/cm^2$ in 0.5BF-yDF-(0.5-y)PT, respectively. The improved Pr value has been discussed in relation with crystal structure and electrical property.

Key words : Ferroelectricity, Ceramics, Rietveld method, Neutron diffraction, $BiFeO_3$-$PbTiO_3$

1. Introduction

The $BiFeO_3$ had drawn interest due to its multifunctional property of ferroelectricity and antiferromagnetism simultaneously in the bulk ceramics. The $BiFeO_3$ (BF) has a G-type antiferromagnetic (T_N = 397°C)[1,2] and has a rhombohedral structure (R3c, a = 5.616 Å, α = 59.35°).[3] The saturation polarization P_s of ferroelectric BF single crystal was 3.5 $\mu C/cm^2$ at liquid nitrogen temperature.[4] Recently, Wang *et al.*[5] reported that epitaxially grown BF thin film exhibits a very large P_s value (P_s = 50~90 $\mu C/cm^2$) and spontaneous magnetization (5~150 emu/cm^3) simultaneously.

Fedulov *et al.*[6] and Smith *et al.*[7] had reported dielectric phase transitions at the temperature range of 450 – 650°C in the (1-x)$BiFeO_3$ (BF)-x$PbTiO_3$ (PT) binary system. They also suggested a phase transition from rhombohedral to tetragonal over the composition range of x = 0.275~0.325. Fedulov *et al.* suggested that this system could be a good candidate for a high temperature piezoelectric material and it would be expedient to introduce a substance to reduce the electrical conductivity of the BF-PT.

In this study we have investigated the crystal structure and ferroelectricity of the BF-PT and BF-DF-PT systems for the purpose of obtaining a high temperature piezoelectric. This study is focused on the relation between crystal structure and ferroelectric property. The DF has been added for reducing electrical conductivity of the BF-PT ceramics. The orthoferrites $ReFeO_3$ (Re = rare earth) are G-type antiferromagnets (T_N = 645~730 K) with weak ferromagnetism and electrically insulating.[8,9]

2. Experimental Procedure

The binary and ternary ceramic samples of (1-x)BF-xPT (x = 0.2~0.6) and xBF-yDF-zPT (x + y + z = 1) have been prepared using the perovskite end members, BF, DF, and PT. Each end members had been prepared from chemically pure PbO, Dy_2O_3, TiO_2, Bi_2O_3, and Fe_2O_3. Calcined powders of each end members were mixed according to the desired compositions and ball-milled with PVA. The mixtures were dried and pressed into discs of 0.9 mm diameter. The pressed samples were sintered at temperature range of 930~1100°C for 5 h in air so as to control the linear sintering shrinkage range oover 14 ± 0.3%.

Hysteresis curves of Polarization-Electric field (P-E) have been measured using RT66A ferroelectric tester of Radiant Technologies. The electrical properties such as the dielectric constant (ε_r), dielectric loss (tan δ), and electrical resistivity (Ω_m) have been also measured. The X-ray diffraction data were obtained at room temperature using a MacScience M18XHF diffractometer. Neutron diffraction data were obtained over the temperature of 293~1203 K using HRPD diffractometer at HANARO in Korea Atomic Energy Research Institute. The neutrons from the HANARO reactor were monochromatized by a vertically focusing composite Ge-monochromator to a wavelength of 1.8348 Å. The crystal structure was analyzed by the rietveld profile refinement method using the program Fullprof.

†Corresponding author : Jeong Seog Kim
E-mail : kimjungs@office.hoseo.ac.kr
Tel : +82-41-540-5921 Fax : +82-41-540-5345

3. Results and Discussion

The P-E hysteresis curves of the binary (1-x) BF-xPT (x = 0.2~0.6) are shown in Fig. 1. The 0.6BF-0.4PT sample shows a relatively large remanant polarization Pr (2 $\mu C/cm^2$). But the other samples (x = 0.2, 0.6) show so small Pr values that cannot be considered as ferroelectric.

The P-E hysteresis curves of the ternary system of the 0.5BF-yDF-(0.5-y) PT (y = 0.05, 0.1, 0.15, 0.2) are shown in Fig. 2. The addition of 0.05 moleDF (y = 0.05) does not produce any significant change in Pr value. At y = 0.1 mole(DF) the Pr drastically increases to 31 $\mu C/cm^2$. With further increase of DF the Pr decreases to 6 $\mu C/cm^2$ at y = 0.2. Fig. 3 shows the P-E curves of 0.6BF-yDF-(0.4-y) PT (y = 0, 0.1, 0.2). The linear P-E curve of the 0.35BF-0.3DF-0.35PT is introduced into Fig. 3 for the comparison to other samples. The largest Pr value (16 $\mu C/cm^2$) is obtained at y = 0.1 similarly to the case of 0.5BF-yDF-(0.5-y)PT system (Fig. 2). With increasing DF to y = 0.2 the Pr decrease to 0.5 $\mu C/cm^2$. The coercive electric field E_c also increases to 35~55 kV/cm

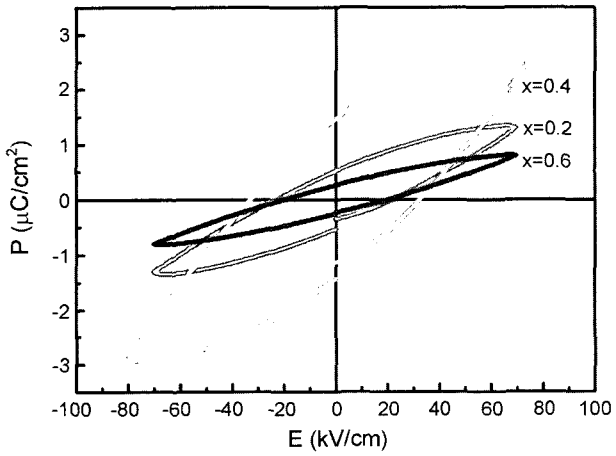

Fig. 1. P-E hysteresis curves of (1-x)BF-xPT system (x = 0.2, 0.4, 0.6) at RT.

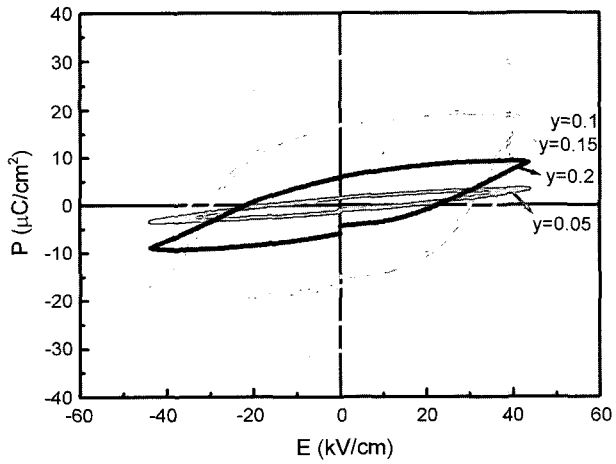

Fig. 2. P-E hysteresis curves of 0.5BF-yDF-(0.5-y)PT system (y = 0.05, 0.1, 0.15, 0.2).

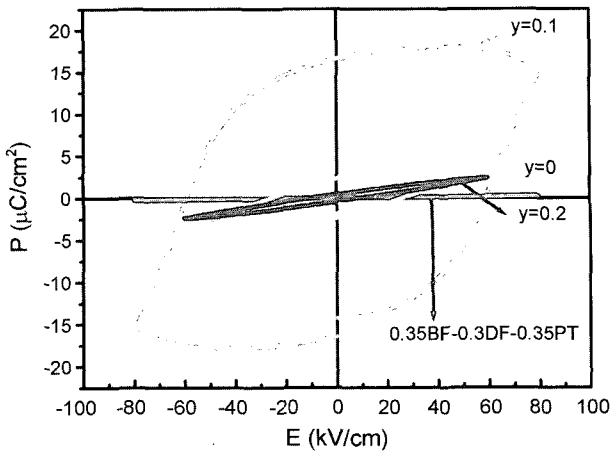

Fig. 3. P-E hysteresis curves of 0.6BF-yDF-(0.4-y)PT system (y = 0.0, 0.1, 0.2) and 0.35BF-0.3DF-0.35PT at RT.

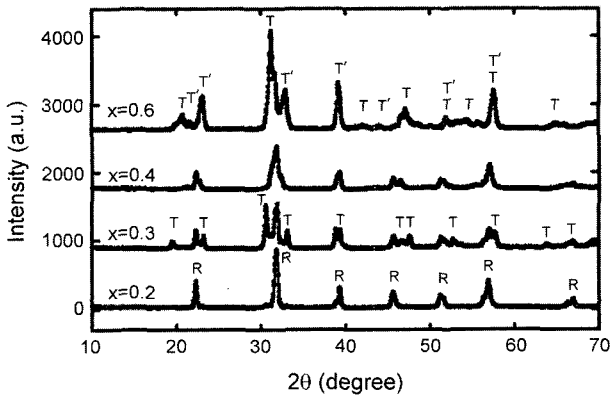

Fig. 4. XRD patterns of the (1-x)BF-xPT (x = 0.2, 0.3, 0.4, 0.6). (R : R-3c, T : P4/mbm, T' : P4mm).

in proportional to the increase of the Pr values.

Fig. 4 shows the XRD patterns of the (1-x)BF-xPT (x = 0.2, 0.3, 0.4, 0.6). The results of crystal structure analysis by rietveld refinement are summarized in Tables 1 and 2. The refinement reliability factors i.e., 'R'-values in Table 1 are fairly large that there remains some uncertainty concerning the space group and atomic positions. But we can derive some meaningful information such as lattice parameters and the type of phases existing in the samples from these refinement results.

The XRD pattern of x = 0.2 shows a pure single phase of rhombohedral structure (marked by R in Fig. 4). At x = 0.3 both a tetragonal (P4/mbm, marked by T) and rhombohedral (R-3c, marked by R) phases coexist. The structural refinement results of 0.6BF-0.4PT showed similar level of 'R'values either by the rhombohedral R-3c or by the orthorhombic Bmmb (a = 7.709 Å, b = 7.726 Å, c = 8.594 Å). The 0.4BF-0.6PT consists of two tetragonal phases, P4/mbm (T) and P4mm (marked by T') as shown in Table 1.

The XRD patterns of the xBF-yDF-zPT [x : y : z = 0.4 : 0.1 : 0.5 (415), 0.5 : 0.05 : 0.45 (50.54.5), 0.6 : 0.1 : 0.3 (613), 0.5 : 0.1 : 0.4 (514)] are shown in Fig. 5. The 514 and 613 show

Table 1. Summary of Rietveld Refinement Results Using X-Ray Diffraction Data of BF-PT System (R : R-3c, T : P4/mbm T' : P4mm, S.G. : space group)

Composition	0.8BF-0.2PT	0.7BF-0.3PT		0.6BF-0.4PT		0.4BF-0.6PT	
S.G.	R-3c	R-3c + P4/mbm		R-3c + P4mm		P4/mbm + P4mm	
a	5.5739(8)	5.5916(12)	5.4054(12)	5.5765(26)	3.8791(13)	5.4594(23)	3.8961(12)
b	5.5739(8)	5.5916(12)	5.4054(12)	5.5765(26)	3.8791(13)	5.4594(23)	3.8961(12)
c(Å)	13.814(3)	13.858 (5)	4.5028(13)	13.727(13)	4.1546(18)	4.3223(52)	4.1183(13)
χ^2	1.82	3.47		2.33		5.07	
R_p, R_{wp}	15.5, 20.4	18.7, 24.4		17.2, 22.5		18.9, 23.9	
R_b, R_f	9.44, 5.87	9.47, 5.68	19.5, 10.9	13.3, 8.43	15.0, 9.70	13.7, 8.52	9.69, 6.57
Phase	R	R ≈ T		R > T'		T > T'	

Table 2. Summary of Rietveld Refinement Results Using Neutron and X-Ray Diffraction Data of 0.5BF-0.1DF-0.4PT

	0.5BF-0.1DF-0.4PT							
	Neutron						XRD	
Temperature	293 K		753 K		953 K		293 K	
S.G.	R-3c	Pm3m	R-3c	Pm3m	R-3c	Pm3m	R-3c	Pm3m
a	5.5867(13)	3.9504(4)	5.6065(6)	3.9665(4)	5.6198(7)	3.9763(4)	5.5861(12)	3.9474(5)
b	"	"	"	"	"	"	"	"
c(Å)	13.685(6)	"	13.754(3)	"	13.792(3)	"	13.682(6)	"
χ^2	2.92	4.32	2.75	2.94	2.37	2.73	7.35	7.64
R_p, R_{wp}	6.70, 8.67	7.83, 10.4	6.12, 8.28	6.07, 8.44	5.87, 7.64	5.74, 8.06	11.1, 15.1	11.4, 14.9
R_b, R_f	14.6, 11.7	20.5, 15.3	13.5, 13.5	14.0, 12.0	15.0, 17.9	12.8, 11.6	9.26, 7.73	10.6, 6.61

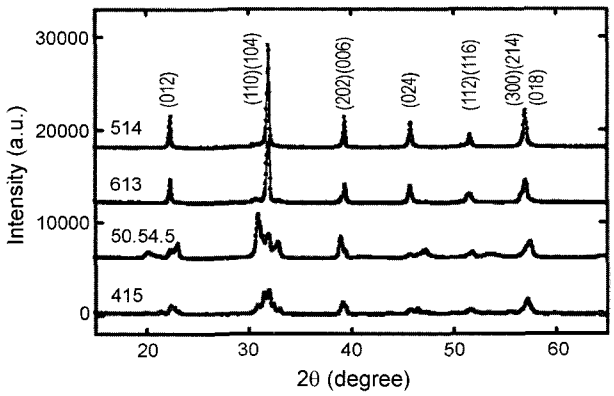

Fig. 5. XRD patterns of xBF-yDF-zPT [x : y : z = 0.4 : 0.1 : 0.5 (415), 0.5 : 0.05 : 0.45 (50.54.5), 0.6 : 0.1 : 0.3 (613), 0.5 : 0.1 : 0.4 (514)] (The reflections are indexed by the R-3c structure).

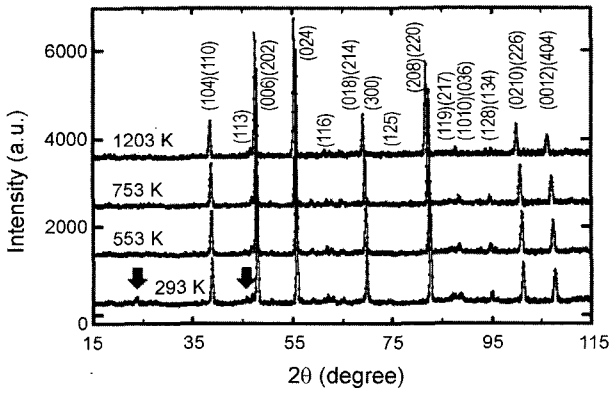

Fig. 6. Neutron diffraction patterns of the 514 at 293 K, 553 K, 753 K, 1203 K. (Reflections are indexed based on the R-3c. Reflections marked by arrows originate from the G-type antiferromagnetic ordering).

the R-3c structure with very small amount of an impurity phase. Contrarily, the 415 and the 50.54 samples consist of at least two phases (the phases marked by R, T, and T' in Fig. 4).

Neutron diffraction patterns of the 514 at the temperature range of 293~1203 K are shown in Fig. 6. The reflections marked by the arrows originate from the G-type antiferromagnetic ordering.[8,9] The structural refinement results using the x-ray and neutron diffraction data are summarized in Table 2. The XRD analysis resulted in the similar R-values either by the noncentrosymmetric R-3c or by the centrosymmetric Pm3m model. However, the refinements using neutron data at 293 K produce smaller R-values from the R-3c model compared to the cubic Pm3m. This neutron data analysis result is in accord to the ferroelectricity observed in the 514 specimen.

Table 4 shows the dielectric constant ε_r, dielectric loss tan δ, and electrical resistivity Ωm for the binary and ternary samples. In the binary (1-x)BF-xPT system the relative dielectric constant ε_r and electrical resistivity Ωm decreases with x. The ε_r increases substantially with the addition of DF as shown in the Table 4. The Ωm of ternary samples decreases slightly compared to those of the binary samples of similar BF contents. Hence the increase of ε_r by the DF addition could be also considered as a contributing factor for the improvement of remanant polarization values.

Table 3. Remanant Polarization Pr and Rhombohedral Angle α

Sample	BF (XRD)	8BF-2PT (XRD)	7BF-3PT (XRD)	6BF-4P (XRD)	6BF-1DF-3PT (XRD)	5BF-1DF-4PT (neutron)	5BF-2DF-3PT. (neutron)	4BF-2DF-4PT (neutron)	4BF-1DF-5PT (XRD)
a_R(Å)	5.6343	5.6177	5.6356	5.5948	5.904	5.5868	5.5883	5.5783	5.6101
α(°)	59.35	59.48	59.48	59.78	60.01	59.99	59.92	60.05	59.72
Pr(μC/cm^2)	-	0.5	-	2.0	17	31	6.2	12	3.7

Table 4. Electrical Properties of the Binary and Ternary Composition Samples

Sample	8BF-2PT (950°C/5Hr)	7BF-3PT (970°C/5Hr)	6BF-4PT (950°C/5Hr)	4BF-6PT (950°C/5Hr)	6BF-2DF-2PT (1020°C/5Hr)	5BF-1DF-4PT (1020°C/5Hr)	4BF-1DF-5PT (1040°C/5Hr)
ε_r	163	173	164	107	285	202	340
tan δ	0.026	0.023	0.051	0.037	0.060	0.020	0.023
Ωm	4.68×10^9	1.88×10^9	1.04×10^9	6.54×10^7	5.73×10^8	3.71×10^7	1.39×10^7

The P-E hysteresis curves in Figs. 2 and 3 show electrically leaky behavior to a certain degree. This leaky behavior leads to an ambiguity when comparing the measured Pr values of the electrically leaky samples. However, the P-E curves in this study are measured under the same test conditions using the using RT66A ferroelectric tester of Radiant Technologies. In addition the electrical resistivity Ωm of ternary samples remain in the same orders of magnitude (~10^{-7} Ωm) compared to those of the binary samples. The unsaturated P-E hysteresis curves are also often found in the electrically leaky samples such as the $SrBi_2Ta_2O_9$ ceramics known for ferroelectric memory material.[10] Therefore, we can derive some meaningful relation from the trial analysis of crystal structure by comparing the Pr values of the binary and ternary samples.

The degree of structural distortion to rhombohedral from a cubic perovskite structure of the rhombohedral phases in the bulk samples has been calculated using the refined structural parameters of the BF-DF-PT. The hexagonal lattice parameters shown in Tables 1 and 2 have been converted to those of the rhombohedral axis (lattice parameter a_R and rhombohedral angle α). The calculated rhombohedral angle α is shown in Table 3. The deviation from 60° represents the distortion to rhombohedral from the cubic. The rhombohedral with $\alpha \approx 60°$ implies a pseudocubic. The BF shows the largest deviation from 60° ($\alpha = 59.35°$). With increasing x in the (1-x)BF-xPT system the α approaches close to 60°. The Pr value shows a maximum value (31 μC/cm^2) at

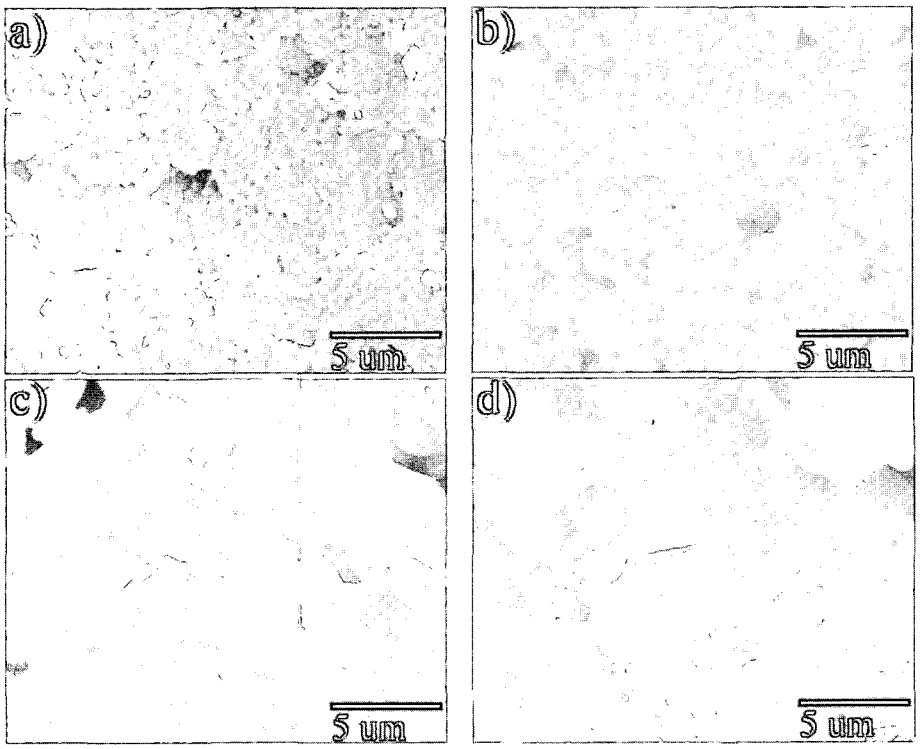

Fig. 7. SEM images of the fractured surfaces of (a) 0.4BF-0.6PT sintered at 1100°C, (b) 0.6BF-0.4PT sintered at 970°C, (c) 613 sintered at 970°C, and (d) 514 sintered at 1000°C.

$\alpha = 59.99°$ and decreases with a deviation from this α value.

The pseudocubic crystal structure of the 514 and 613 ($\alpha \approx 60°$) can lead to an easy domain wall motion during the ferroelectric polarization and hence can be ascribed to the origin of the superior Pr values.[11,12] On the other hand the retardation of domain wall motion by the lattice strain can lead to the decrease of the Pr values with the deviation from $\alpha = 60°$.

The effect of grain size is another important aspect worthwhile to discuss concerning the superior ferroelectricity of the 514 and 613 samples. The scanning electron micrographs of the fracture surfaces of the sintered samples (0.4BF-0.6PT, 0.6BF-0.4PT, 613, 514) are shown in Fig. 7. The addition of DF into the binary BF-PT system expedites the grain growth. The 514 showing the largest Pr value has the largest grain size (~4 μm). The grain size effect on the Pr has been well reported in PZT and other ferroelectric materials.[13,14] Presently we would like to suggest that all the three aspects discussed above can be the candidates for the origin of the enhanced Pr value. Further study needs to be done for clarifying these effects.

4. Conclusions

The effect of DF addition has been investigated on the crystal structure and ferroelectricity over the phase boundary region in the (1-x)BF-xPT system. The DF addition drastically enhanced the ferroelectric property. The Pr reaches a maximum value at y = 0.1 in the 0.6BF-yDF-(0.4-y)PT and 0.5BF-yDF-(0.5-y)PT systems, 17 $\mu C/cm^2$ and 31 $\mu C/cm^2$ respectively. Both the 613 and 514 samples with superior Pr values have a rhombohedral R-3c structure of a pseudo-cubic nature. The DF addition resulted in the expedited grain growth and the increase of dielectric constant ε_r while the resistivity Ω_m and tan δ remaining in similar level of values compared to the binary system.

Acknowledgment

This work was supported by the research fund of Hoseo University in 2004.

REFERENCES

1. I. Sosnowska, T. Peterlin-Neumaier, and E. Strichele, "Spiral Magnetic Ordering in Bismuth Ferrite," *J. Phys. C: Solid State Phys.*, **15** 4835-46 (1982).
2. S. V. Kiselev, R. P. Ozerov, and G. S. Zhdanov, "Detection of Magnetic Order in Ferroelectric $BiFeO_3$ by Neutron Diffraction," *Sov. Phys.-Doklady*, **7** [8] 742-44 (1963).
3. F. Kubel and H. Schmid, "Structure of a Ferroelectric and Ferroelastic Monodomain Crystal of the Perovskite $BiFeO_3$," *Acta Cryst.*, **B46** 698-702 (1990).
4. J. R. Teague, R. Gerson, and W. J. James, "Dielectric Hysteresis in Single Crystal $BiFeO_3$," *Solid State Commun.*, **8** 1073-74 (1970).
5. J. Wang, J. B. Neaton, H. Zheng, V. Nagarajan, S. B. Ogale, B. Lie, D. Vieland, V. Vaithyanathan, D. G. Sholm, U. V. Waghmare, N. A. Spaldin, K. M. Rabe, M. Wuttig, and R. Ramesh, "Epitaxial $BiFeO_3$ Multiferroic Thin Film Heterostructures," *Science*, **229** 1719-22 (2003).
6. S. A. Fedulov, P. B. Ladyzhinskii, I. L. Pyatigorskaya, and Y. N. Venevtsev, "Complete Phase Diagram of the $PbTiO_3$-$BiFeO_3$ System," *Sov. Phys.-Sol. St.*, **6** [2] 375-78 (1964).
7. R. T. Smith, G. D. Achenbach, R. Gerson, and W. J. James, "Dielectric Properties of Solid Solutions of $BiFeO_3$ with Pb(Ti, Zr)O_3 at High Temperature and High Frequency," *J. Appl. Phys.*, **39** [1] 70-4 (1968).
8. J. S. Kim, C. I. Cheon, Y. N. Choi, and P. W. Jang, "Ferroelectric and Ferromagnetic Properties of $BiFeO_3$-$PrFeO_3$-$PbTiO_3$ Solid Solutions," *J. Appl. Phys.*, **93** 9263-70 (2003).
9. W. P. Wolf and R. L. White, "Rare-Earth Compounds," *J. Appl. Phys.*, **40** [3] 1061-69 (1969).
10. C. I. Cheon and J. S. Kim, "Ferroelectric Properties of Ti-Doped and W-Doped SBT Ceramics(*in Korean*)," *J. Kor. Ceram. Soc.*, **41** [5] 401-05 (2004).
11. C. I. Cheon and H. G. Kim, "Ferroelectric Domain Structure and Array of Tetragonal and Rhombohedral Phase in PZT Ceramics at MPB Composition(*in Korean*)," *J. Kor. Ceram. Soc.*, **30** [11] 919-24 (1993).
12. D. M. Kim, J. S. Kim, and C. I. Cheon, "Effects of Particle Size on Properties of PZT-Based Thick Films(*in Korean*)," *J. Kor. Ceram. Soc.*, **41** [5] 375-80 (2004).
13. H. T. Chung and H. G. Kim, "The Effects of Tetragonality to the Physical Properties of PZT(*in Korean*)," *J. Kor. Ceram. Soc.*, **24** [1] 56-62 (1987).
14. T. Yamamoto, K. Okazaki, M. L. Dass, and G. Thomas, "Microstructure and the Dielectric Properties at the Morphotropic Phase Boundary (MPB) of $PbTiO_3$-$PbZrO_3$ System," *Ferroelectrics*, **81** 331-34 (1988).